SHORT COMMUNICATION

Cal-520FF is the Present Optimal Ca^{2+} Indicator for Ultrafast Ca^{2+} Imaging and Optical Measurement of Ca^{2+} Currents

Laila Ananda Blömer [1,2] · Luiza Filipis [1,2] · Marco Canepari [1,2,3] (ID)

Abstract

Ultrafast Ca^{2+} imaging using low-affinity fluorescent indicators allows the precise measurement of the kinetics of fast Ca^{2+} currents mediated by voltage-gated Ca^{2+} channels. Thus far, only a few indicators provided fluorescence transients with sufficient signal-to-noise ratio necessary to achieve this measurement, with Oregon Green BAPTA-5N exhibiting the best performance. Here we evaluated the performance of the low-affinity Ca^{2+} indicator Cal-520FF to record fast Ca^{2+} signals and to measure the kinetics of Ca^{2+} currents. Compared to Oregon Green BAPTA-5N and to Fluo4FF, Cal-520FF offers a superior signal-to-noise-ratio providing the optimal characteristics for this important type of biophysical measurement. This ability is the result of a relatively high fluorescence at zero Ca^{2+}, necessary to detect enough photons at short exposure windows, and a high dynamic range leading to large fluorescence transients associated with short Ca^{2+} influx periods. We conclude that Cal-520FF is at present the optimal commercial low-affinity Ca^{2+} indicator for ultrafast Ca^{2+} imaging applications.

Introduction

Fluorescence dyes with low-affinity ($K_D \geq 10$ μM) for Ca^{2+} allow measuring intracellular Ca^{2+} transients with minimal perturbation of physiological conditions [1]. Furthermore, the relaxation time of the Ca^{2+}-dye binding reactions for these indicators is considerably shorter than that for high-affinity ($K_D < 1$ μM) indicators [2]. This property allows the temporal tracking of fast Ca^{2+} influx through voltage-gated Ca^{2+} channels (VGCCs) and therefore the possibility to precisely measure the kinetics of the Ca^{2+} current [3, 4]. In the dendrites of hippocampal CA1 pyramidal neurons [5], the Ca^{2+} current kinetics associated with an action potential (AP) can be directly measured by calculating the time-derivative of the fractional change of fluorescence ($\Delta F/F_0$). Alternatively, the estimate of Ca^{2+} current kinetics can be generalised by taking into account the competing interaction of Ca^{2+} with the endogenous buffers [6]. Thus far and after testing several low-affinity indicators, we have established that the best performing indicator for this type of application, in terms of signal-to-noise ratio (SNR), was Oregon Green BAPTA-5N (OG5N, $K_D \sim 35$ μM). We used this indicator to measure the kinetics of Ca^{2+} currents in CA1 hippocampal pyramidal neurons [5], in cerebellar Purkinje neurons [7, 8] and in olfactory bulb mitral cells [9]. Fura-FF ($K_D \sim 10$ μM) is another low-affinity fluorescent indicator, with different spectral properties, that is suitable for this type of measurement, with the advantage of allowing simultaneous fluorescence measurements of the membrane potential [10]. Its performance in terms of SNR, however, is inferior with respect to the great performance of OG5N. It was shown that the high-affinity green fluorescent indicator Cal-520 performed significantly better than several other indicators with similar affinity in terms of SNR [11]. Hence, we decided to test the performance of its low-affinity equivalent Cal-520FF (Cal520FF, $K_D \sim 10$ μM) with the prospective of possibly adopting this indicator for ultrafast Ca^{2+} imaging. To this purpose, we comparatively analysed the performance of Cal520FF with respect to the two green low-affinity fluorescent indicators Fluo-4FF (Fluo4FF, $K_D \sim 10$ μM) and OG5N. Whereas OG5N was our indicator of reference, the choice of

✉ Marco Canepari
marco.canepari@univ-grenoble-alpes.fr

1 University Grenoble Alpes, CNRS, LIPhy, F-38000 Grenoble, France

2 Laboratories of Excellence, Ion Channel Science and Therapeutics, Valbonne, France

3 Institut National de la Santé et Recherche Médicale, Paris, France

Fluo4FF was motivated by the fact that this indicator, unlike OG5N, has very dim fluorescence at zero Ca^{2+}, but a much larger dynamic range with respect to OG5N. Thus, we could quantitatively position the performance of Cal520FF with respect to the different characteristics of the two indicators of comparison.

Materials and Methods

For all comparative tests on Fluo4FF (Thermo Fisher Scientific, Waltham, MA, USA), Cal520FF (AAT Bioquest, Sunnyvale, CA, USA) and OG5N (Thermo Fisher Scientific), we used a set-up originally developed for fast Ca^{2+} imaging [3]. The system was mounted on an Olympus BX51 microscope equipped for electrophysiology in brain slices and with a 60X NA = 1 objective. Fluorescence was excited at 470 nm using an OptoLED system (CAIRN Research Ltd., Faversham, UK) and recorded at 530 ± 21 nm with a NeuroCCD-SMQ camera (RedShirtimaging, Decatur, GA, USA). Each indicator was purchased in its (potassium) salt form and dissolved in an aqueous solution. Physiological tests were performed in somatosensory neocortical layer-5 (L5) pyramidal neurons from brain slices prepared as described in a recent publication [12]. Briefly, animal manipulation was ethically carried out in accordance with European Directives 2010/63/UE on the care, welfare and treatment of animals and procedures were reviewed by the ethics committee affiliated to the animal facility of the university (D3842110001). 21–35 postnatal days old mice (C57BL/6j) were anesthetised by isofluorane inhalation and brain slices (350 μm thick) with an orientation of 15 degrees from the coronal plane were prepared using a Leica VT1200 vibratome (Leica, Wetzlar, Germany). The extracellular solution used to maintain the slices and for perfusion during the experiment contained (in mM): 125 NaCl, 26 $NaHCO_3$, 1 $MgSO_4$, 3 KCl, 1 NaH_2PO_4, 2 $CaCl_2$ and 20 glucose, bubbled with 95 % O_2 and 5 % CO_2. After slicing, slices were incubated for ~ 30 minutes at 37 ºC and left 1 h at room temperature before starting the experiments. Slices were transferred to the recording chamber and continuously perfused at 32–34 ºC. Individual neurons were loaded with an indicator by establishing patch clamp whole cell recordings using a Multiclamp 700A (Molecular Devices, Sunnyvale, CA). Cells were dialysed with an intracellular solution containing (in mM): 125 $KMeSO_4$, 5 KCl, 8 $MgSO_4$, 5 Na_2-ATP, 0.3 Tris-GTP, 12 Tris-Phosphocreatine, 20 HEPES adjusted to pH 7.35 with KOH, and 2 mM of one Ca^{2+} indicator. Recordings started 30 minutes after establishing the whole cell in order to assure the dye equilibration. The patch clamp electrode was also used to elicit and record an AP and the membrane potential (V_m) corrected for the bridge and the junction potential (-11 mV). Ca^{2+} fluorescence measurements were performed at 20 kHz and Ca^{2+} transients were expressed

as fractional changes of fluorescence ($\Delta F/F_0$). Full names of organic VGCC inhibitors (from Tocris, Bristol, UK) were Isradipine: 4-(2,1,3-Benzoxadiazol-4-yl)-1,4-dihydro-2,6-dimethyl-3,5-pyridinecarboxylic acid methyl 1-methylethyl ester; ML218: 3,5-dichloro-N-[[(1α,5α,6-exo,6α)-3-(3,3-dimethylbutyl)-3-azabicyclo[3.1.0]hex-6-yl]methyl]-benzamide-hydrochloride; NNC550396: (1S,2S)-2-[2-[[3-(1H-Benzimidazol-2-yl)propyl]methylamino]ethyl]-6-fluoro-1,2,3,4-tetrahydro-1-(1-methylethyl)-2-naphthalenyl-cyclopropanecarboxylate-dihydrochloride. ω-Agatoxin IVA, ω-Conotoxin GVIA and SNX482 were purchased from Smartox Biotechnology (St Martin d'Hères, France).

Results

The SNR increases linearly with the sensitivity of the indicator, but it also increases with the square root of the basal fluorescence, which is close to the zero Ca^{2+} fluorescence. Thus, we initially evaluated the three low-affinity Ca^{2+} indicators Fluo4FF, OG5N and Cal520FF, with respect to these parameters. We prepared three solutions (1 mL each) containing 100 mM HEPES, buffered to pH 7.35 with KOH, 5 mM EGTA (to set 0 mM Ca^{2+}) and 80 μM of either Fluo4FF, OG5N or Cal520FF. We then evaluated each solution at zero Ca^{2+} separately in the microscope chamber by measuring the fluorescence excited with a light spot of ~ 100 μm diameter using the CCD camera (Fig. 1a). As expected, at zero Ca^{2+}, Fluo4FF had dim fluorescence quantified by 164 digits of the CCD camera, OG5N had brighter fluorescence quantified by 1455 digits and Cal520FF had intermediate fluorescence quantified by 785 digits. Next, we evaluated the dynamic range of each indicator by adding to each solution 10 μL of 1 M $CaCl_2$, to increase Ca^{2+} to ~ 5 mM in this way saturating the indicators (Fig. 1b). The maximal fluorescence, normalised to the zero Ca^{2+} fluorescence, was 89, 35, and 62 for Fluo4FF, OG5N and Cal520FF respectively. Finally, to evaluate the SNR performance that can be predicted in a physiological Ca^{2+} measurement, we calculated the product of the square root of the zero Ca^{2+} fluorescence (Fig. 1a) times the full dynamic range (Fig. 1b). As shown in Fig. 1c, OG5N performs better in terms of SNR than the dim Fluo4FF, but Cal520FF can potentially perform better than both indicators.

With this premise, we evaluated the performance of the three indicators in measuring the fast Ca^{2+} transient associated with an AP in L5 pyramidal neurons from acute brain slices (Fig. 2a) and the ability to reconstruct the underlying Ca^{2+} current by calculating the time-derivative of the Ca^{2+} $\Delta F/F_0$ signal. Individual neurons were loaded with a Ca^{2+} indicator using whole cell patch clamp recordings (Fig. 2b) as described in the Materials and Methods. The Ca^{2+} $\Delta F/F_0$ signal associated with an AP was used for this test. This signal is mediated
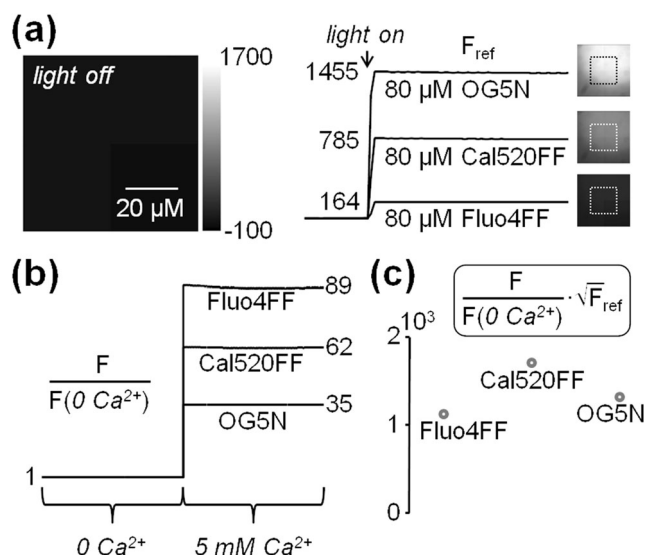
Fig. 1 Evaluation of the three low-affinity indicators Fluo4FF, OG5N and Cal520FF. **a** Left: field of view of the CCD camera; frame acquired without illumination. Right, three sequences of images acquired from a solution containing zero Ca^{2+} and 80 μM of either Fluo4FF (bottom), OG5N (top) or Cal520FF (middle); traces report the light intensity on the square region before and after turning on the 470 nm LED for the three indicators; the images are illustrated on the same greyscale to appreciate the different zero Ca^{2+} fluorescence levels; the values of the CCD digits in the three cases are reported. **b** In the three solutions of panel a, Ca^{2+} was increased from 0 to 5 mM and the ratio between the maximal and minimal Ca^{2+} (dynamic range) was calculated: 89 for Fluo4FF; 35 for OG5N; 62 for Cal520FF. (**c**) The product of the dynamic range (panel b) and of the square root of the CDD digits corresponding to zero Ca^{2+} (panel a): 1140 for Fluo4FF; 1335 for OG5N; 1737 for Cal520FF

by diverse VGCCs (L-type, P/Q-type, N-type, R-type and T-type) and it is locally blocked by a cocktail of VGCC inhibitors (20 μM Isradipine, 1 μM ω-Agatoxin IVA, 1 μM ω-Conotoxin GVIA, 1 μM SNX482, 5 μM ML218, 30 μM NNC550396) as shown in the example of Fig. 2a. For each indicator, 10 neurons were loaded with 2 mM of either Fluo4FF, Cal520FF or OG5N. We recorded the fluorescence time-course associated with an AP along a proximal segment of the apical dendrite and calculated the Ca^{2+} $\Delta F/F_0$ signal from regions located at 80–100 μM from the soma at 20 kHz (Fig. 2b). Notably, in each cell tested, the loading conditions were standardised, fluorescence was excited at the same intensity and the auto-fluorescence was subtracted in order to accurately measure F_0. In each cell, we also averaged 9 recordings, and we corrected each trace for bleaching. In the three examples of Fig. 2b, F_0 was the dimmest for Fluo4FF and the brightest for OG5N whereas the maximum $\Delta F/F_0$ after the AP was the largest for Fluo4FF and the smallest for OG5N. As expected from the preliminary analysis reported in Fig. 1, for both F_0 and the maximum $\Delta F/F_0$, Cal520FF gave intermediate values with respect to the other two indicators. But when visually examining the normalised signals, Cal520FF exhibited the largest SNR among the three indicators. To quantify and assess the consistency of this result, for the three groups of 10

cells, we measured F_0, the maximum $\Delta F/F_0$ and the SNR quantified by the ratio between the maximum $\Delta F/F_0$ and the $\Delta F/F_0$ standard deviation calculated from the samples before the AP (Fig. 2c). By applying either a parametric ANOVA test, or a non parametric Kruskal-Wallis test, the three groups resulted significantly different for the three parameters analysed ($p < 0.001$) and Cal520FF signals had the largest SNR among the three indicators.

The importance of ultrafast Ca^{2+} imaging relies on the ability of tracking the kinetics of fast VGCCs by precisely reconstructing the shape of the Ca^{2+} current, which can be obtained in pyramidal neuron dendrites by calculating the time-derivative of the $\Delta F/F_0$ signal. Thus, we estimated the Ca^{2+} current kinetics by filtering fluorescence with a 20-points Savitsky-Golay smoothing filter and by calculating the time-derivative (dF/dt) of the filtered fluorescence, as shown for the three examples in Fig. 2d. As in the case of the $\Delta F/F_0$ signal, the SNR of the dF/dt signal was visually larger in the example with Cal520FF. The SNR for the three groups of cells was then calculated for dF/dt (Fig. 2d). Again, for this signal, Cal520FF gave the largest SNR as revealed by the same two tests used above ($p < 0.001$). In summary, the significantly highest performance of Cal520FF in ultrafast Ca^{2+} imaging makes this relatively new indicator the most ideal, at present, for this type of applications.

Discussion

Low-affinity Ca^{2+} indicators are used when the preservation of physiological signalling is necessary or when measuring large Ca^{2+} transients such as those produced by release from internal stores (see for example [13]). In addition, whereas high-affinity Ca^{2+} indicators still provide meaningful information in the acquisition frequency range of 100–1000 Hz [14–16], acquiring fluorescence from low-affinity Ca^{2+} indicators in the kHz range allows measuring the kinetics of fast Ca^{2+} currents [3–6]. As for other fluorescence functional signals, the bottle-neck for using these indicators for a particular measurement is the achievable SNR. This limitation is critical in the case of neuronal fast Ca^{2+} imaging where the number of collected photons is set by the short exposure time of the camera, but also by the necessary spatial resolution. Up to now, the outstanding SNR of OG5N allowed fast confocal measurements of Ca^{2+} signals at 1.25 kHz from dendritic spines [17] and ultrafast (non-confocal) measurements of Ca^{2+} signals at 20 kHz from dendrites, leading to the measurement of native Ca^{2+} currents [8]. The selection of OG5N followed a series of unpublished examinations where several low-affinity Ca^{2+} indicators with different spectral properties were tested, including Fura, Fluo, Oregon Green and Rhod indicators. The analysis reported here demonstrates now a significantly better performance of the green fluorescent indicator Cal520FF with respect to OG5N,
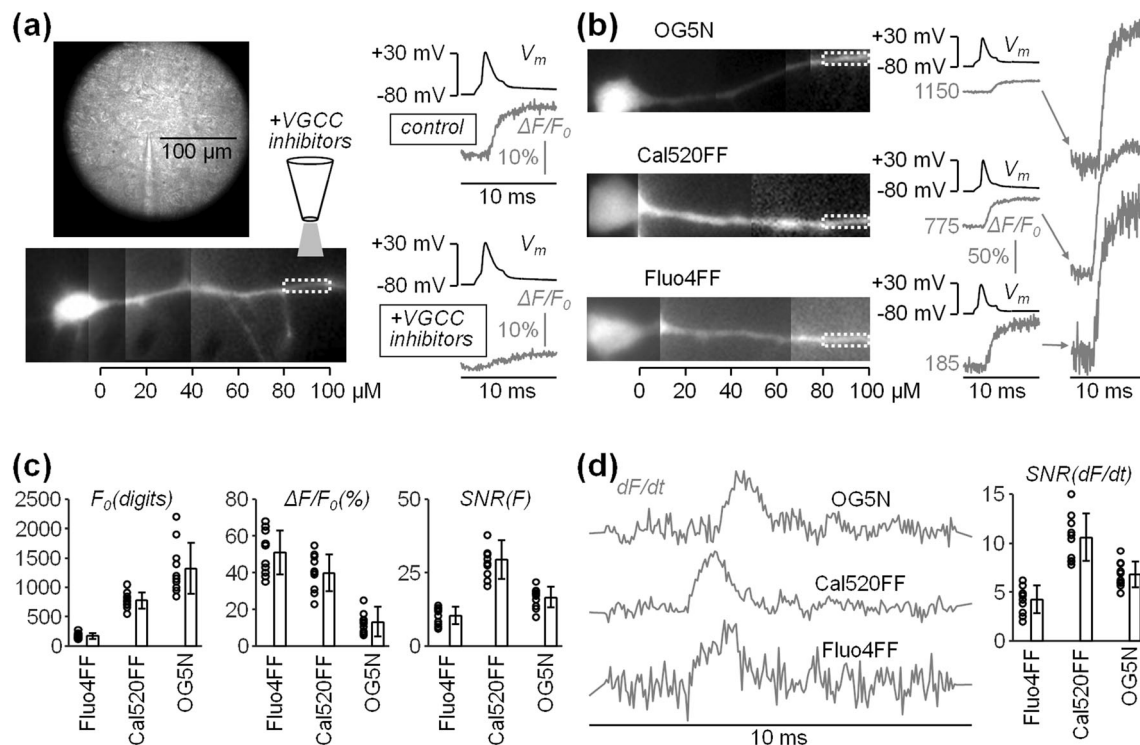
Fig. 2 Performance of Fluo4FF, OG5N and Cal520FF for ultrafast Ca^{2+} imaging and optical recording of Ca^{2+} currents. **a** Image of a brain (cortical) slice with patched L5 pyramidal neuron. On the bottom, a fluorescence image of a neuron loaded with 2 mM OG5N with a region of interest (white-dotted rectangle) indicated; a pipette locally delivering a cocktail of VGCC inhibitors (see main text) is drawn to indicate its position. On the right, somatic V_m with evoked AP and associated $\Delta F/F_0$ Ca^{2+} signal in control condition and after locally delivering the VGCC inhibitors showing the block of the Ca^{2+} transient and no effect on the somatic AP. **b** Left: fluorescence images of L5 pyramidal neurons loaded with 2 mM of either Fluo4FF (bottom), Cal520FF (middle) or OG5N (top); the white-dotted rectangles outline the regions (80–100 μm from the soma) from where fluorescence was averaged. Centre, $\Delta F/F_0$ signals (grey) associated with an AP (black); the camera digits corresponding to F_0 are indicated. Right, the normalised $\Delta F/F_0$ signals showing the different SNR. **c** Left, F_0 values (digits) in 10 cells for each indicator and mean ± SD for Fluo4FF (174 ± 48), Cal520FF (780 ± 139) and OG5N (1325 ± 425). Centre, maximum $\Delta F/F_0$ (%) values in the 10 cells and mean ± SD for Fluo4FF (51 ± 12), Cal520FF (40 ± 10) and OG5N (13 ± 8). Right, $\Delta F/F_0$ SNR values in the 10 cells and mean ± SD for Fluo4FF (10.3 ± 3.0), Cal520FF (29.5 ± 6.6) and OG5N (16.5 ± 3.5). **d** Left, normalised time-derivative of F after smoothing (dF/dt) in the three cells of panel a. Right, dF/dt SNR values in the 10 cells and mean ± SD for Fluo4FF (4.2 ± 1.4), Cal520FF (10.5 ± 2.4) and OG5N (6.8 ± 1.3). All data are from averages of 9 trials

extending the improved characteristics of its high-affinity equivalent Cal-520 [11]. Combining a relatively high fluorescence at zero Ca^{2+} with a dynamic range that is nearly twice of that of OG5N, the resulting larger SNR of Cal520FF overcomes the performance of all other commercial indicators.

Declarations

Consent to Participate Not applicable.

Consent for Publication Not applicable.

Conflict of Interest The authors declare neither conflicts of interest nor competing interests.

References

1. Hyrc KL, Bownik JM, Goldberg MP (2000) Ionic selectivity of low-affinity ratiometric calcium indicators: mag-Fura-2, Fura-2FF and BTC. Cell Calcium 27:75–86. https://doi.org/10.1054/ceca.1999.0092

2. Kao JP, Tsien RY (1988) Ca2+ binding kinetics of fura-2 and azo-1 from temperature-jump relaxation measurements. Biophys J 53:635–639. https://doi.org/10.1016/S0006-3495(88)83142-4

3. Jaafari N, De Waard M, Canepari M (2014) Imaging fast calcium currents beyond the limitations of electrode techniques. Biophys J 107:1280–1288. https://doi.org/10.1016/j.bpj.2014.07.059

4. Jaafari N, Marret E, Canepari M (2015) Using simultaneous voltage and calcium imaging to study fast $^{2+}$ channels. Neurophotonics 2: 021010. https://doi.org/10.1117/1.NPh.2.2.021010

5. Jaafari N, Canepari M (2016) Functional coupling of diverse voltage-gated Ca(2+) channels underlies high fidelity of fast dendritic Ca(2+) signals during burst firing. J Physiol 594:967–983. https://doi.org/10.1113/JP271830

6. Ait Ouares K, Jaafari N, Canepari M (2016) A generalised method to estimate the kinetics of fast Ca(2+) currents from Ca(2+) imaging experiments. J Neurosci Methods 268:66–77. https://doi.org/10.1016/j.jneumeth.2016.05.005

7. Ait Ouares K, Filipis L, Tzilivaki A, Poirazi P, Canepari M (2019) Two distinct sets of Ca2 + and K + channels are activated at different membrane potentials by the climbing fiber synaptic potential in purkinje neuron dendrites. J Neurosci 39:1969–1981. https://doi.org/10.1523/JNEUROSCI.2155-18.2018

8. Ait Ouares K, Canepari M (2020) The origin of physiological local mGluR1 supralinear Ca^{2+} signals in cerebellar Purkinje neurons. J Neurosci 40:1795–1809. https://doi.org/10.1523/JNEUROSCI.2406-19.2020

9. Ait Ouares K, Jaafari N, Kuczewski N, Canepari M (2020) Imaging native calcium currents in brain slices. Adv Exp Med Biol 1131:73–91. https://doi.org/10.1007/978-3-030-12457-1_4

10. Vogt KE, Gerharz S, Graham J, CanepariM (2011) High-resolution simultaneous voltage and Ca^{2+} imaging. J Physiol 589, 489–494. https://doi.org/10.1113/jphysiol.2010.200220

11. Lock JT, Parker I, Smith IF (2015) A comparison of fluorescent Ca^{2+} indicators for imaging local Ca^{2+} signals in cultured cells. Cell Calcium 58:638–648. https://doi.org/10.1016/j.ceca.2015.10.003

12. Filipis L, Canepari M (2020) Optical measurement of physiological sodium currents in the axon initial segment. J Physiol. https://doi.org/10.1113/JP280554

13. Khodakhah K, Ogden D (1995) Fast activation and inactivation of inositol trisphosphate-evoked Ca^{2+} release in rat cerebellar Purkinje neurones. J Physiol 487:343–358. https://doi.org/10.1113/jphysiol.1995.sp020884

14. Canepari M, Mammano F (1999) Imaging neuronal calcium fluorescence at high spatio-temporal resolution. J Neurosci Methods 87: 1–11. https://doi.org/10.1016/s0165-0270(98)00127-7

15. Mammano F, Canepari M, Capello G, Ijaduola RB, Cunei A, Ying L, Fratnik F, Colavita A (1999) An optical recording system based on a fast CCD sensor for biological imaging. Cell Calcium 25:115–123. https://doi.org/10.1054/ceca.1998.0013

16. Canepari M, Mammano F, Kachalsky SG, Rahamimoff R, Cherubini E (2000) GABA- and glutamate-mediated network activity in the hippocampus of neonatal and juvenile rats revealed by fast calcium imaging. Cell Calcium 2725–2733. https://doi.org/10.1054/ceca.1999.0086

17. Filipis L, Ait Ouares K, Moreau P, Tanese D, Zampini V, Latini A, Bleau C, Bleau C, Graham J, Canepari M (2018) A novel multisite confocal system for rapid Ca2 + imaging from submicron structures in brain slices. J Biophotonics 11(3). https://doi.org/10.1002/jbio.201700197